Distinct intramolecular interactions regulate autoinhibition of vinculin binding in αT-catenin and αE-catenin

Jonathon A. Heier[1] ⓘ, Sabine Pokutta[2,3], Ian W. Dale[1], Sun Kyung Kim[4], Andrew P. Hinck[4] ⓘ, William I. Weis[2,3], and Adam V. Kwiatkowski[1],* ⓘ

From the [1]Department of Cell Biology, University of Pittsburgh School of Medicine, Pittsburgh, Pennsylvania, USA; [2]Department of Structural Biology, [3]Department of Molecular and Cellular Physiology, Stanford University, Stanford, California, USA; [4]Department of Structural Biology, University of Pittsburgh School of Medicine, Pittsburgh Pennsylvania, USA

Edited by Enrique De La Cruz

α-Catenin binds directly to β-catenin and connects the cadherin–catenin complex to the actin cytoskeleton. Tension regulates α-catenin conformation. Actomyosin-generated force stretches the middle (M)-region to relieve autoinhibition and reveal a binding site for the actin-binding protein vinculin. It is not known whether the intramolecular interactions that regulate epithelial (αE)-catenin binding are conserved across the α-catenin family. Here, we describe the biochemical properties of testes (αT)-catenin, an α-catenin isoform critical for cardiac function and how intramolecular interactions regulate vinculin-binding autoinhibition. Isothermal titration calorimetry showed that αT-catenin binds the β-catenin–N-cadherin complex with a similar low nanomolar affinity to that of αE-catenin. Limited proteolysis revealed that the αT-catenin M-region adopts a more open conformation than αE-catenin. The αT-catenin M-region binds the vinculin N-terminus with low nanomolar affinity, indicating that the isolated αT-catenin M-region is not autoinhibited and thereby distinct from αE-catenin. However, the αT-catenin head (N- and M-regions) binds vinculin 1000-fold more weakly (low micromolar affinity), indicating that the N-terminus regulates the M-region binding to vinculin. In cells, αT-catenin recruitment of vinculin to cell–cell contacts requires the actin-binding domain and actomyosin-generated tension, indicating that force regulates vinculin binding. Together, our results show that the αT-catenin N-terminus is required to maintain M-region autoinhibition and modulate vinculin binding. We postulate that the unique molecular properties of αT-catenin allow it to function as a scaffold for building specific adhesion complexes.

The cadherin–catenin complex that forms the core of the adherens junction (AJ) is required for intercellular adhesion and tissue integrity (1–3). Classical cadherins are single-pass transmembrane proteins with an extracellular domain that forms *trans*-interactions with cadherins on adjacent cells (4–6). The adhesive properties of classical cadherins are driven by the recruitment of cytosolic catenin proteins to the cadherin tail: p120-catenin binds to the juxtamembrane domain,

and β-catenin binds to the distal part of the tail. β-Catenin recruits α-catenin, a mechanoresponsive actin-binding protein (7–13). The AJ mechanically couples and integrates the actin cytoskeletons between cells to allow dynamic adhesion and tissue morphogenesis (3).

The best characterized member of the α-catenin family of proteins is mammalian epithelial (αE)-catenin. Structurally, it is composed of 5 four-helix bundles connected to a C-terminal five-helix bundle by a flexible linker (14–16). The two N-terminal four-helix bundles form the N-domain that binds β-catenin and mediates homodimerization (12, 17–19). The central 3 four-helix bundles form the middle (M)-region that functions as a mechanosensor (20–25). The C-terminal five-helix bundle forms the F-actin-binding domain (ABD) (11, 13, 26, 27). F-actin binding is allosterically regulated: αE-catenin can bind F-actin readily as a homodimer, but when in complex with β-catenin, mechanical force is required for strong F-actin binding (9–11, 26). In addition, when tension is applied to αE-catenin, salt bridge interactions within the M-region are broken, allowing the domain to unfurl and reveal cryptic binding sites for other cytoskeletal binding proteins such as vinculin (16, 23–25, 28–32). The recruitment of these proteins is thought to help stabilize the AJ in response to increased tension and further integrate the actin cytoskeleton across cell–cell contacts (24, 28, 31, 33–35).

Three α-catenin family proteins are expressed in mammals: the ubiquitous αE-catenin, neuronal (αN)-catenin, and testes (αT)-catenin (36, 37). αE-catenin and αN-catenin are 81% identical and 91% similar in amino acid sequence. αT-catenin is 58% identical and 77% similar to αE-catenin and αN-catenin, making it the most divergent of the family (36–38). αT-catenin is predominantly expressed in the heart, testes, brain, and spinal cord (39, 40). In the heart, it localizes to the intercalated disc (ICD), a specialized adhesive structure that maintains mechanical coupling and chemical communication between cardiomyocytes (41, 42). In mice, loss of αT-catenin from the heart causes dilated cardiomyopathy, and mutations in αT-catenin are linked to arrhythmogenic ventricular cardiomyopathy in humans (43, 44). In addition to cardiomyopathy, αT-catenin is linked to multiple human diseases, including asthma, neurological disease, and cancer (40, 45, 46).

---

* For correspondence: Adam V. Kwiatkowski, adamkwi@pitt.edu.

Despite a growing awareness of its importance in human disease, the molecular properties and ligand interactions of αT-catenin remain poorly understood. Our previous work revealed that αT-catenin, unlike mammalian αE-catenin, is a monomer in the solution that can bind to F-actin with low micromolar affinity in the absence of tension. F-actin binding is also not allosterically regulated, as the β-catenin–αT-catenin complex binds to F-actin with the same affinity as the αT-catenin monomer (38). Single-molecule pulling experiments have shown the αT-catenin M-region to be mechanoresponsive as it unfurls in a force range similar to αE-catenin (47).

Here we show that αT-catenin associates with the components of the cadherin–catenin complex with an affinity similar to αE-catenin *in vitro*, revealing that they may compete with one another for binding β-catenin at the plasma membrane. We also show that the M-region of αT-catenin is not autoinhibited and can bind the vinculin N-terminus in the absence of tension with strong affinity. Unlike αE-catenin, however, when the N-terminus of αT-catenin is attached to the M-region, the affinity for vinculin drops significantly. This indicates that interdomain interactions between the N-terminus and the M-region of αT-catenin regulate its interaction with vinculin. We measured the recruitment of vinculin to cell–cell contacts and found that, despite the distinct mechanism of regulation, recruitment of vinculin is still tension dependent. Our findings indicate that the way in which tension regulates vinculin binding differs between αE-catenin and αT-catenin. We postulate that this mechanism is important for the ability of αT-catenin to build specific and distinct molecular complexes at AJs.

Results

αT-catenin binds tightly to the β-catenin–N-cadherin core complex

We characterized the interaction between αT-catenin and β-catenin by isothermal titration calorimetry (ITC) using purified recombinant proteins. We used the head region (comprising the N- and M-domains) of αT-catenin (aa 1–659, Fig. 1A) for these experiments because it is more stable than full-length αT-catenin and yields sufficiently high protein concentrations for ITC. Past studies revealed that the αE-catenin head region (aa 1–651) binds β-catenin and the β-catenin–E-cadherin tail complex with a similar affinity to full-length αE-catenin (12). We observed that the αT-catenin head binds β-catenin with a dissociation constant ∼250 nM (Fig. 1B; Table 1). The affinity of αT-catenin for β-catenin is an order of magnitude weaker than the association of αE-catenin or αN-catenin for β-catenin (15–20 nM; (12)).

Cadherin tail binding to β-catenin strengthens the affinity between β-catenin and α-catenin (12). N-cadherin is the primary classical cadherin expressed in cardiomyocytes (48). We tested if the N-cadherin tail (Ncad$_{cyto}$) influences the
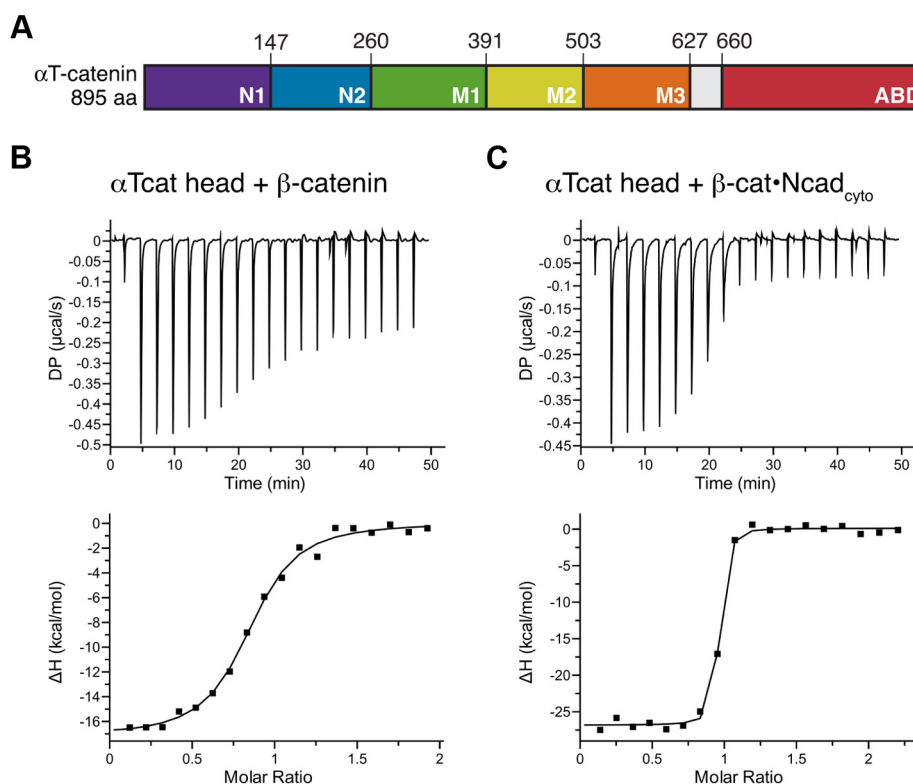
Figure 1. αT-catenin binds the N-cadherin–β-catenin complex with nanomolar affinity. *A*, domain organization of αT-catenin. Amino acid domain boundaries marked. *B* and *C*, αT-catenin head region (aa 1–659, αT-catenin head) binding to β-catenin (*B*) or the β-catenin–N-cadherin cytoplasmic tail (β-catenin–Ncad$_{cyto}$) complex (*C*) was measured by ITC. The ratio of heat released (kcal) per mole of β-catenin or β-catenin–Ncad$_{cyto}$ injected into αT-catenin head was plotted against the molar ratio of αT-catenin head and β-catenin or αT-catenin head and β-catenin–Ncad$_{cyto}$. Thermodynamic properties derived from these traces are shown in Table 1. ITC, isothermal titration calorimetry; Ncad$_{cyto}$, N-cadherin tail.

Table 1
ITC measurements of αT-catenin fragments binding to β-catenin or β-catenin–N-cadherin cytoplasmic tail complex

Proteins	K_d (nM)	ΔH (kcal/mol)	TΔS (kcal/mol)	ΔG (kcal/mol)	#
αT-catenin head (1–659) + β-catenin	264.1 ± 109.1	−14.6 ± 2.1	−5.6	−9.0	5
αT-catenin head (1–659) + β-catenin–Ncad$_{cyto}$	5.6 ± 0.6	−27.0 ± 0.2	−15.8	−11.3	3
αT-catenin N1-N2 (1–259) + β-catenin–Ncad$_{cyto}$	6.9 ± 12.0	−18.9 ± 1.0	−7.8	−11.1	1

Ncad$_{cyto}$, N-cadherin tail.

αT-catenin–β-catenin interaction by titrating the β-catenin–Ncad$_{cyto}$ complex into αT-catenin head (Fig. 1C). The affinity of this interaction was 5 to 6 nM (Table 1), indicating that αT-catenin binds to the cadherin–β-catenin complex an order of magnitude more strongly than to β-catenin alone. This affinity is similar to the 1- to 2-nM affinity observed between the cadherin tail–β-catenin complex and αE-catenin or αN-catenin (12) and suggests that αT-catenin can effectively compete with αE-catenin for binding to the membrane-associated cadherin–β-catenin complex.

αT-catenin N-terminus is monomeric

Full-length αT-catenin is primarily a monomer in the solution, although it does have homodimerization potential *in vitro* (38). The best evidence for dimerization potential
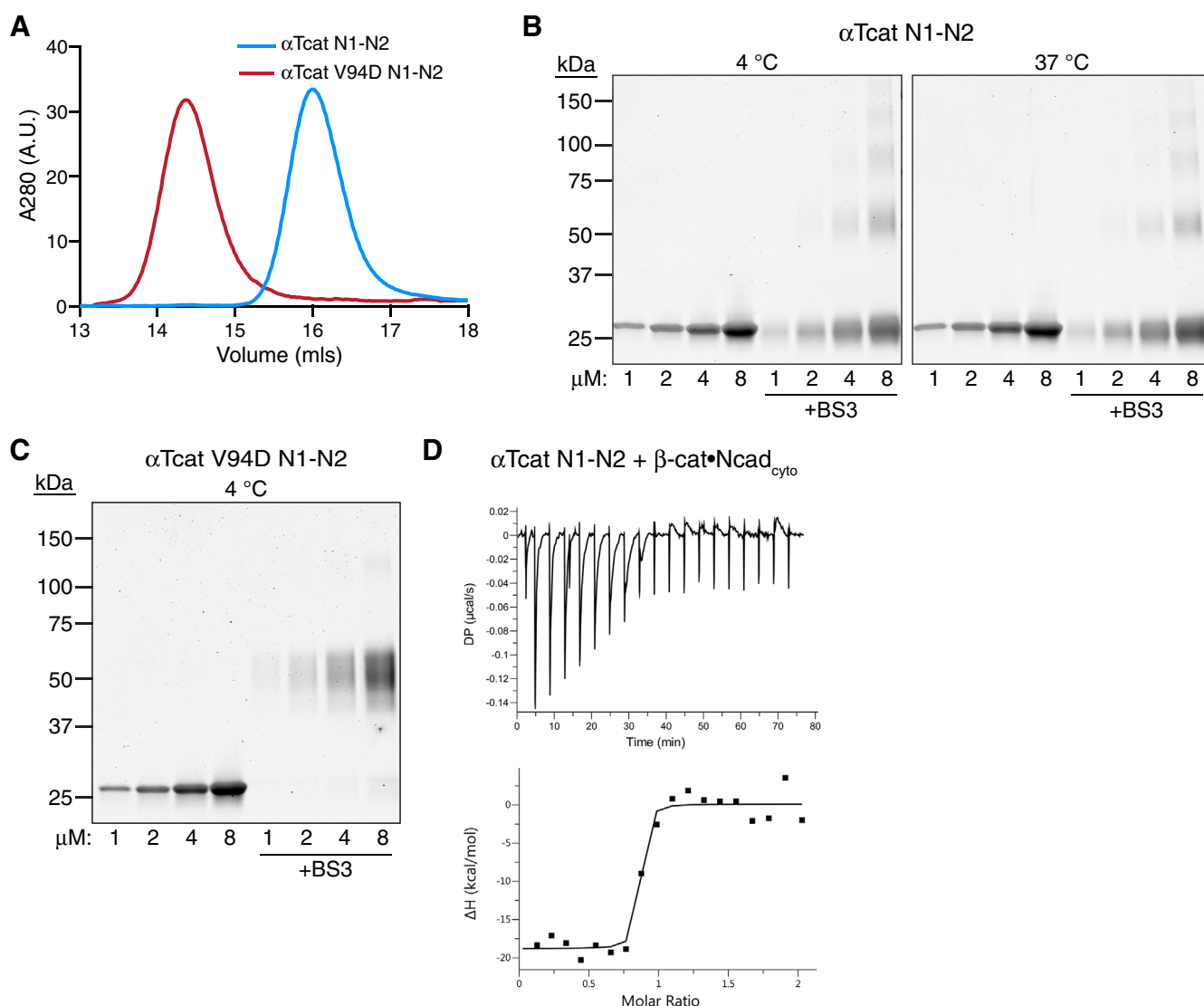
Figure 2. αT-catenin N1-N2 is a monomer in the solution. *A*, analytical SEC of 30-μM αT-catenin N1-N2 (aa 1–259, *blue line*) and 30-μM αT-catenin V94D N1-N2 (*red line*). *B*, crosslinking experiments with αT-catenin N1-N2. Increasing concentrations of αT-catenin were incubated with or without 1-mM BS3 at 4 °C (*left panel*) or 37 °C (*right panel*) for 30 min, separated by SDS-PAGE and stained with the Coomassie dye. *C*, crosslinking experiments of αT-catenin V94D N1-N2. Increasing concentrations of αT-catenin V94D N1-N2 were incubated with or without 1-mM BS3 at 4 °C for 30 min, separated by SDS-PAGE, and stained with Coomassie dye. *D*, αT-catenin N1-N2 binding to β-catenin–N-cadherin cytoplasmic tail (β-cat–Ncad$_{cyto}$) was measured by ITC. Thermodynamic properties derived from this trace are shown in Table 1. ITC, isothermal titration calorimetry; Ncad$_{cyto}$, N-cadherin tail; SEC, size-exclusion chromatography.

comes from a point mutation linked to arrhythmogenic ventricular cardiomyopathy in humans, V94D, that renders αT-catenin an obligate homodimer (38, 44). We analyzed the oligomerization properties of the αT-catenin N1-N2 (aa 1–259, Fig. 1A) and compared them to the V94D mutant. Analytical size-exclusion chromatography of αT-catenin WT N1-N2 and V94D N1-N2 revealed that WT N1-N2 eluted as a single monomer species (Fig. 2A, *blue line*), whereas the V94D mutant eluted as a dimer species (Fig. 2A, *red line*).

We then analyzed the oligomeric state of the αT-catenin N-terminus by cross-linking. Increasing concentrations of αT-catenin N1-N2 were incubated with or without the cross-linker bis(sulfosuccinimidyl)suberate (BS3) at 4 °C or 37 °C and the resulting products analyzed by SDS-PAGE. As expected, the αT-catenin N1-N2 migrated as a 25-kDa protein in the absence of a cross-linker (Fig. 2B). Incubation with BS3 did not affect migration at low concentrations, although at higher concentrations (4 and 8 μM), larger species were detected at both temperatures. In contrast, αT-catenin V94D N1-N2 ran as 50-kDa protein in the presence of BS3 at all concentrations tested (Fig. 2C), indicating a cross-linked dimer. We conclude that the αT-catenin N terminus, similar to full-length protein, is primarily a monomer in the solution.

We then tested the ability of the αT-catenin N1-N2 to bind to the β-catenin–Ncad$_{cyto}$ complex by ITC. The affinity of this interaction was 7 nM (Fig. 2D, Table 1), similar to the αT-catenin head and confirming that this fragment contains the complete β-catenin binding site.
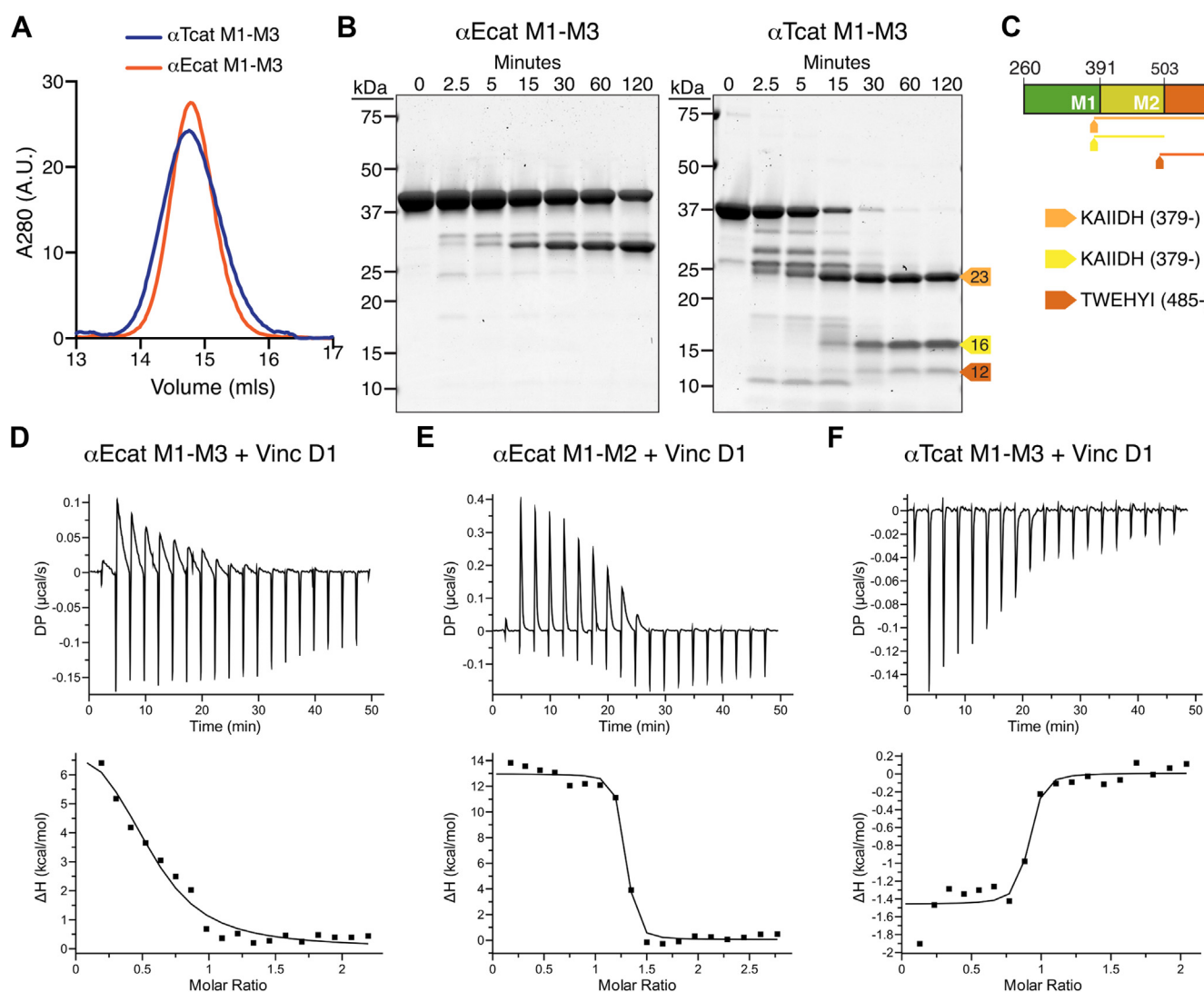
Figure 3. αT-catenin M1-M3 binds vinculin D1 with high affinity. *A*, analytical SEC of recombinant αT-catenin M1-M3 (aa 260–626) and αE-catenin M1-M3 (aa 273–651). *B*, limited proteolysis of αT-catenin and αE-catenin M1-M3 fragments. Proteins incubated for 0, 2.5, 5, 15, 30, 60, and 120 min at room temperature in 0.05 mg/ml trypsin, resolved by SDS-PAGE, and stained with the Coomassie dye. Stable fragments of 23 (*yellow-orange*), 16 (*yellow*), and 12 kDa (*orange*) are marked with *colored arrows*. *C*, Edman sequencing results of limited proteolysis fragments. Protein fragments are mapped on the M1-M3 sequence as *color-coded lines*. *D–F*, representative ITC traces of αE-catenin M1-M3 (*D*), αE-catenin M1-M2 (aa 273–510, *E*), and αT-catenin M1-M3 (*F*) binding to vinculin D1 (aa 1–259). Thermodynamic properties derived from these traces are shown in Table 2. ITC, isothermal titration calorimetry; SEC, size-exclusion chromatography.

αT-catenin M-region binds vinculin

The αE-catenin M region is autoinhibited with respect to vinculin binding: mechanical force is required to break an internal salt bridge network within M1-M3 to reveal the vinculin-binding site in M1 (25, 30). The αT-catenin M region also recruits vinculin and force is required to unfurl M1 to promote high-affinity binding (47). However, our previous proteolysis experiments of full-length αT-catenin revealed that the M2-M3 region existed in a more open, protease-sensitive state (38). Notably, the amino acids that form the salt bridges required for autoinhibition in the αE-catenin M-region are conserved in αT-catenin, with the exception of E277 in M1 that pairs with R451 in M2. In αT-catenin, the arginine is conserved at the corresponding residue (aa 446), but the glutamic acid is replaced by a threonine at aa 272 (25), preventing these residues from interacting. We questioned if αT-catenin M1-M3 adopted an autoinhibited conformation.

We examined the organization and vinculin-binding properties of the complete αT-catenin M-region (M1-M3, aa 260–626). αT-catenin M1-M3 eluted as a single, discrete peak by size-exclusion chromatography, identical to αE-catenin M1-M3 (aa 273–651; Fig. 3A). We then probed the M-region flexibility by limited trypsin proteolysis. Tryptic digestion of αE-catenin M1-M3 revealed that it was largely protease resistant: nearly 50% of the fragment was still intact after 120 min of digestion, consistent with it forming a closed, autoinhibited domain (Fig. 3B). In contrast, αT-catenin M1-M3 was completely digested after 60 min into three stable fragments at 23, 16, and 12 kDa (Fig. 3B). Note that both M regions contain a similar number of lysine and arginine residues (47 in αE-catenin and 39 in αT-catenin), the majority of which are conserved. N-terminal sequencing revealed that the 23-kDa and 16-kDa fragments both started at aa 379 and represented the M2-M3 and M2 bundles, respectively. The 12-kDa fragment started at aa 485 and corresponded to the M3 bundle (Fig. 3C). Similar protease-resistant fragments were observed from digest of full-length protein (38) and are consistent with the αT-catenin M-region adopting a more open, protease-sensitive state relative to αE-catenin, despite five of the six salt bridge residue pairs being conserved. Likewise, the isolated αT-catenin M1-M3 fragment does not appear to adopt a stable, autoinhibited conformation.

We then measured the affinity of αT-catenin M1-M3 for vinculin. We used the vinculin D1 fragment (aa 1–259) that contains the first 2 four-helix bundles and binds to αE-catenin

with a similar affinity to the vinculin head domain, D1-D4 (23). As observed previously (23), the autoinhibited αE-catenin M1-M3 fragment bound weakly to vinculin D1 (Fig. 3D, Table 2). When M3 was deleted from this fragment, autoinhibition was relieved and αE-catenin M1-M2 bound to vinculin with low nanomolar affinity, as observed previously (Fig. 3E, Table 2) (23). In contrast, the αT-catenin M1-M3 fragment showed strong, nanomolar binding to vinculin D1 similar to αE-catenin M1-M2 (Fig. 3F, Table 2), indicating that αT-catenin M1-M3 binding to vinculin was not autoinhibited. Whereas binding to αE-catenin M1-M2 or M1-M3 is endothermic (entropy driven), consistent with unfolding of the M1 bundle needed for this interaction (23), binding to αT-catenin M1-M3 was exothermic, suggesting that αT-catenin M1 is unfurled in the M1-M3 fragment.

αT-catenin N-terminus regulates vinculin binding

Recent *in vitro* single-molecule stretching experiments revealed that force is required to expose the vinculin-binding site in αT-catenin M1-M3 (47). However, our ITC results with the αT-catenin M1-M3 fragment indicated that tension was not required to release M1. In the stretching experiments, the αT-catenin M1-M3 fragment was flanked by a pair of titin I27 immunoglobulin-like domains, and the N-terminus of the fusion protein was tethered to a substrate (47). We questioned if N-terminal associations with M1-M3 stabilize M1 and regulate vinculin binding.

We first characterized the interaction between αT-catenin head domain and vinculin D1 by ITC. The binding shifted from exothermic to endothermic, and the affinity was ∼5 μM, two orders of magnitude weaker than those observed with M1-M3 (Fig. 4A, Table 2). This suggested that the addition of N1-N2 stabilized M1 and inhibited vinculin binding.

Recent work revealed allosteric coupling between the N-terminal domains and M-region of αE-catenin (16). Specifically, the presence of β-catenin caused changes in the accessibility of cysteine residues in the N2–M2 interface and in M3. Because β-catenin binding alters the relative positions of the αE-catenin N1 and N2 domains (12), we tested if β-catenin binding to the αT-catenin N-region affected vinculin binding to the M-region. Vinculin D1 was titrated into a solution of the purified αT-catenin head–β-catenin complex. The presence of β-catenin had little impact on the affinity (∼3 μM, Fig. 4B, Table 2), indicating that N-terminal-mediated autoinhibition was maintained. This result is consistent with past work

Table 2

ITC measurements of αT-catenin and αE-catenin M-domain fragments binding to vinculin D1

Proteins	K_d (nM)	ΔH (kcal/mol)	TΔS (kcal/mol)	ΔG (kcal/mol)	#
αE-catenin M1-M3 (273–651) + vinculin D1	10,420 ± 4588.4	12.8 ± 5.2	19.6	−6.8	3
αE-catenin M1-M2 (273–510) + vinculin D1	31.9 ± 9.1	8.7 ± 0.2	18.9	−10.3	2
αT-catenin M1-M3 (260–626) + vinculin D1	60.5 ± 19.2	−2.2 ± 1.0	13.8	−9.8	3
αT-catenin head (1–659) + vinculin D1	4690 ± 2740	2.3 ± 1.3	9.6	−7.3	2
αT-catenin head (1–659)–β-catenin + vinculin D1	2770 ± 875	4.4 ± 0.6	11.9	−7.5	1
αT-catenin N2-M3 (147–626) + vinculin D1	50.2 ± 40.4	4.0 ± 0.1	14.1	−10.1	3
I27-αT-catenin M1-M3 (260–626) + vinculin D1	245.3 ± 39.7	4.8 ± 0.3	13.8	−9.0	3
αT-catenin N1-N2 (1–259)/M1-M3 (260–626) + vinculin D1	50.1 ± 17.5	−3.1 ± 0.1	6.9	−10.0	2

ITC, isothermal titration calorimetry.

showing that the β-catenin–cadherin complex had no effect on αE-catenin binding to vinculin (23).

We then asked if the entire N-terminus is required to regulate M1 binding. The addition of N2 to αT-catenin M1-M3 (aa 147–626) did not weaken vinculin D1 binding relative to M1-M3 (K_d = 50 nM, Fig. 4*C*, Table 2). The reaction switched from exothermic to endothermic, suggesting partial compensation of M1 stability in this fragment. Thus, all or part of N1 is required to regulate M1 interactions with vinculin. This is consistent with the observation that removing the first 56 residues of N1 from full-length αE-catenin reduces the inhibition of vinculin binding by about 50-fold (23).

We next questioned if the titin repeats attached to M1-M3 in the construct used by Pang *et al.* (47) stabilized M1. We titrated vinculin D1 into a solution of the 2I27–αT-catenin M1-M3 (aa 259–667)-2I27 construct. Notably, the binding was endothermic and the affinity was ∼250 nM, markedly weaker than that observed with αT-catenin M1-M3 alone (Fig. 4*D*, Table 2). We speculate that the well-structured titin repeats promote M1 stability and may sterically occlude vinculin D1 binding, thus reducing the affinity. The M1 stability and steric hindrance provided by the I27 repeats partially mimic the complete N-terminus and likely explain why tension is needed to promote vinculin binding in the single-molecule stretching experiments, whereas αT-catenin M1-M3 in the solution binds vinculin readily.

Given that the entire N-terminus is required to regulate vinculin binding in αT-catenin, we asked if N1-N2 could regulate M1-M3 in *trans*. We titrated vinculin D1 into an equimolar mixture of αT-catenin N1-N2 and M1-M3. The binding reaction was similar to M1-M3 alone: exothermic with a K_d of 50 nM (Fig. 4*E*, Table 2). This result indicates that the M-region must be physically coupled to the N-terminus to stabilize M1 and regulate ligand accessibility.

Tension recruits vinculin to αT-catenin

We tested the ability of αT-catenin to restore cell–cell adhesion and recruit vinculin in α-catenin-deficient R2/7 carcinoma cells (49). We transiently expressed enhanced green fluorescent protein (EGFP)–αE-catenin or EGFP–αT-catenin in R2/7 cells and analyzed cell–cell contact formation and endogenous vinculin recruitment by immunostaining. Both EGFP–αE-catenin and EGFP–αT-catenin restored cell–cell adhesion, organized F-actin along cell–cell contacts, and recruited vinculin to junctions (Fig. 5). To determine if vinculin recruitment was tension dependent, we treated cells with dimethyl sulfoxide or 50-μM blebbistatin to suppress myosin activity for 30 min and stained for vinculin (Fig. 5, *A–D*). αE-catenin and αT-catenin recruited similar levels of vinculin in dimethyl sulfoxide controls (Fig. 5, *A*, *B* and *E*). Importantly, blebbistatin treatment significantly reduced vinculin recruitment to both αE-catenin and αT-catenin containing AJs (Fig. 5, *C–E*). Thus, myosin-based tension is required to recruit vinculin to αT-catenin, similar to αE-catenin.

We then examined the correlation between EGFP fusion expression and vinculin recruitment. As expected, EGFP–αE-

catenin expression levels did not correlate with vinculin levels because vinculin was only recruited when αE-catenin was activated by sufficient tension (24, 28). However, we observed a positive correlation between EGFP–αT-catenin expression and vinculin recruitment. We observed a similar positive correlation with constitutively open αE-catenin constructs in cardiomyocytes (34). Together, these results suggest that while vinculin recruitment to αT-catenin is tension dependent, the force threshold for binding may be low, permitting all/most AJ-incorporated αT-catenin molecules to recruit vinculin.

Finally, we tested if actin binding was required to relieve αT-catenin autoinhibition and if removal of M3 opened the M-region to permit vinculin recruitment. We expressed EGFP-tagged truncations of αE-catenin and αT-catenin: the head domain lacking the ABD (N1-M3) or the head domain minus M3 and ABD (N1-M2). All EGFP-tagged αE-catenin and αT-catenin fragments expressed as soluble proteins of the predicted size (Fig. 5*N*). αE-catenin and αT-catenin N1-M3 (aa 1–670 and aa 1–659, respectively) were both cytosolic and, as expected, unable to form cell–cell contacts and recruit vinculin (Fig. 5, *J* and *K*). Deletion of M3 in αE-catenin relieves autoinhibition, and αE-catenin N1-M2 (aa 1–510) was able to recruit vinculin and restore cell–cell adhesion, as shown previously (49). Here vinculin provides the necessary actin-binding activity to link the cadherin–catenin complex to F-actin through αE-catenin. In contrast, αT-catenin N1-M2 (aa 1–502) was cytosolic and failed to recruit vinculin to cell–cell contacts. This suggests that in αT-catenin, loss of M3 does not release M1 for ligand binding and underscores the importance of the N-terminus in regulating M1 binding to vinculin.

Discussion

αT-catenin forms a strong AJ core with cadherin–β-catenin

Our ITC results show that the β-catenin–Ncad$_{cyto}$ complex binds with high, ∼5-nM affinity to αT-catenin similar to 1- to 2-nM affinity previously reported between the β-catenin–cadherin tail complex and αE-catenin (12). Thus, αT-catenin forms a strong cadherin–catenin core complex like αE-catenin to link actin to the AJ. αT-catenin is coexpressed with αE-catenin in multiple mammalian tissues and, in the heart, it is enriched along the ICD with αE-catenin (39, 45, 46, 50). It is unknown if αE-catenin and αT-catenin bind stochastically to the cadherin–β–catenin complex in cardiomyocytes or if binding is regulated to favor one α-catenin or the other. Notably, loss of either αE-catenin or αT-catenin from the mouse heart causes dilated cardiomyopathy (43, 51), suggesting that each α-catenin has a unique, critical role in ICD function and heart physiology. In addition, αE-catenin and αT-catenin (Heier and Kwiatkowski, unpublished data) also bind plakoglobin, the desmosome-associated β-catenin homolog that is enriched at the ICD (52, 53). Plakoglobin binds the cadherin tail with an affinity similar to β-catenin, and both plakoglobin and β-catenin are enriched at cardiomyocyte AJs (50). The downstream consequences of α-catenin binding to plakoglobin or β-catenin are not clear, but recent evidence that the N-terminus and M-region of αE-catenin are allosterically

coupled (16) raises the possibility that differential binding could affect downstream ligand recruitment. Future work is expected to reveal how specific cadherin–β-catenin/plakoglobin–α-catenin complexes are formed and function to regulate adhesion and signaling.

In the absence of the cadherin tail, β-catenin alone binds αT-catenin an order of magnitude weaker than αE-catenin (∼250 nM *versus* ∼20 nM). This suggest that αT-catenin does not compete with αE-catenin for binding cytosolic β-catenin. Although there is evidence of a cytosolic αE-catenin–β-catenin complex in epithelial cells (54), the physiological relevance of this interaction is not clear and a similar α-catenin–β-catenin complex in cardiomyocytes has not been reported.

αE-catenin can homodimerize and the cadherin-free, cytosolic homodimer pool regulates actin dynamics and cell motility (9, 10, 12, 54, 55). In contrast, full-length αT-catenin is a monomer in the solution and has limited dimerization potential with no evidence of homodimerization *in vivo* (38). Our results here show that the isolated αT-catenin N-terminus is also monomeric. We speculate that limited dimerization potential and weaker affinity for β-catenin favor a cadherin-free, cytosolic pool of an αT-catenin monomer. The role of such a monomer pool is unclear.

The αT-catenin M-region does not adopt an autoinhibited conformation in isolation

Structural, biochemical, and biophysical data indicate that the αE-catenin M-region adopts an autoinhibited conformation (16, 23–25, 28–32). The vinculin binding site is buried in the folded M1 domain, and interactions between M1, M2, and
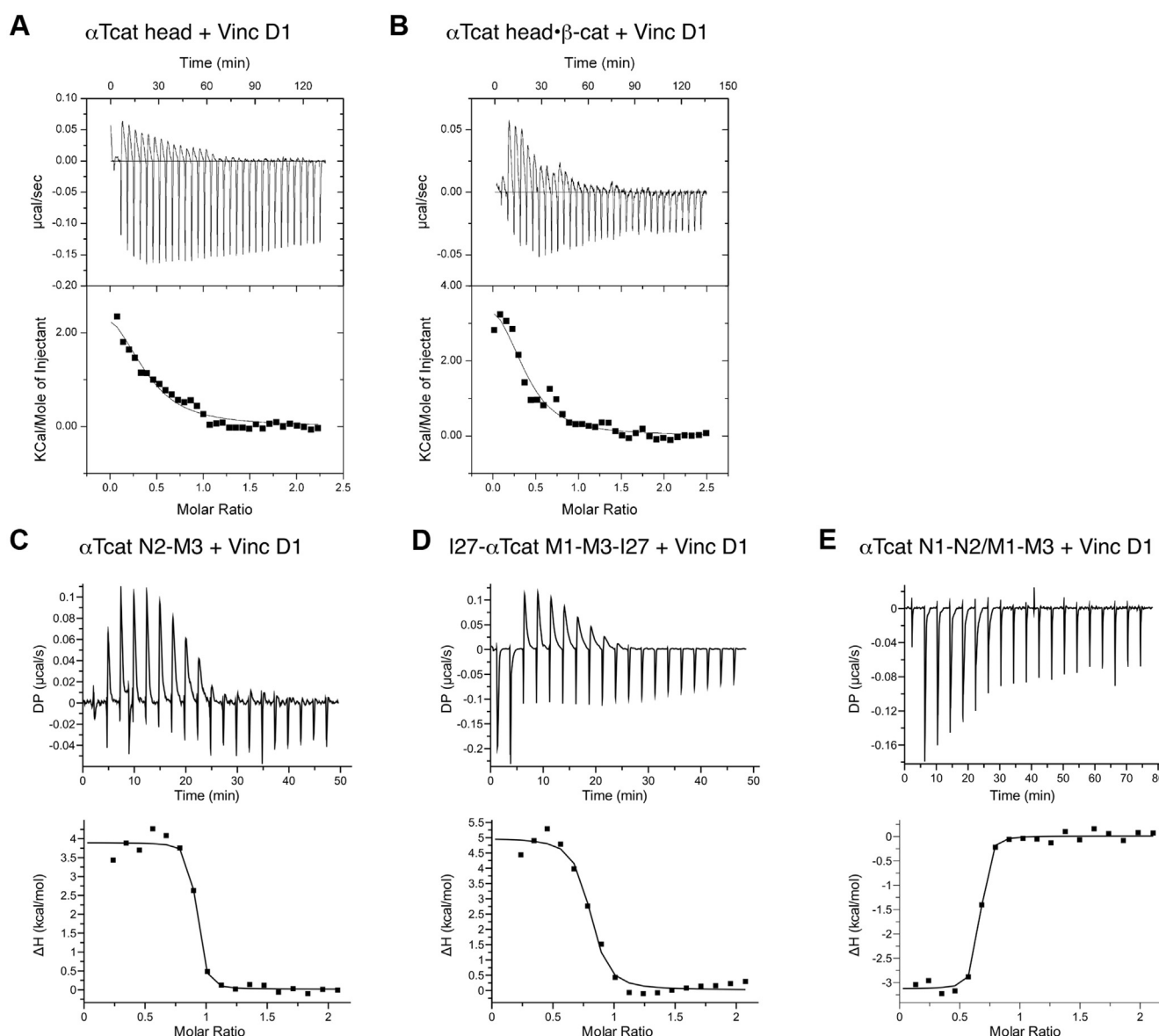
Figure 4. αT-catenin N terminus regulates vinculin binding to M1-M3. *A–D*, representative ITC traces of vinculin D1 binding to αT-catenin head (*A*), αT-catenin head–β-catenin complex (*B*), αT-catenin N2-M3 (aa 147–626, *C*), 2I27-αT-catenin M1-M3 (aa 259–667)-2I27 (*D*), and αT-catenin N1-N2/M1-M3 complex (*E*). Thermodynamic properties derived from these traces are shown in Table 2. ITC, isothermal titration calorimetry.

Figure 5. αT-catenin recruitment of vinculin to cell–cell contacts is tension dependent. *A–D*, R2/7 cells were transfected with EGFP–αE-catenin full length (αEcat FL; *A* and *C*) or EGFP–αT-catenin full length (αTcat FL; *B* and *D*) and treated for 30 min with dimethyl sulfoxide (*A* and *B*) or 50-μM blebbistatin (*C* and *D*) before fixation. Cells were stained for F-actin and vinculin. Individual and merged vinculin (*magenta*) and GFP (*green*) channels are shown. *E*, quantification of vinculin intensity at cell–cell contacts. Signal intensity at contacts was divided by the average cytoplasmic intensity, and a scatter plot of all data points is shown. The *black horizontal line* is the median, and the error bars define the interquartile range. One-way ANOVA with Tukey's comparisons; n ≥ 24 images from two independent experiments. *F–I*, vinculin contact/cytoplasmic ratio (C/C) was plotted against the average GFP intensity of each fusion construct from the masked cell contact region. Linear regression analysis was performed to calculate the slope (*red line*), 95% confidence intervals (*black lines* surrounding the slope), and R^2 value. The slope deviation from zero was analyzed for significance (*p* value). n ≥ 24 images from two independent experiments. *J–M*, R2/7 cells were transfected with EGFP-tagged αE-catenin head (aa 1–670, *J*), αT-catenin head (aa 1–659, *K*), αE-catenin N1-M2 (aa 1–510, *L*), and αT-catenin N1-M2 (aa 1–502, *M*), fixed and stained for vinculin. Individual GFP (*top panel*) and vinculin (*bottom panel*) channels are shown. Scale bar is 10 μm in all images. *N*, R2/7 cells transfected with EGFP-tagged αE-catenin or αT-catenin full-length (FL), head, or N1-M2 constructs. Cell lysates separated by SDS-PAGE and blotted for GFP (*top*) or GAPDH (*bottom*). n.s., not significant.

M3 maintain the autoinhibited form. Tension breaks these interactions to release M1, allowing it to unfold and bind strongly to vinculin. More recent biophysical data suggest that the αT-catenin M-region adopts a similar conformation with force being required to free M1 for high-affinity binding to vinculin (47).

Our limited proteolysis experiments with the isolated αT-catenin M-region indicate that it exists in a more open, protease-sensitive conformation. Consistent with this, ITC results revealed that the αT-catenin M-region binds vinculin with low nanomolar affinity and is not autoinhibited. αT-catenin possesses five of the six residue pairs that form the salt bridge network that mediates αE-catenin autoinhibition (25). The E277-R451 bridge between M1 and M2 in αE-catenin is not conserved in αT-catenin, with the glutamic acid replaced by a threonine at aa 272. The threonine at aa 272 is conserved across the αT-catenin family. Assuming no major structural differences between the αE-catenin and αT-catenin M-regions, the T272 and R446 residues would not be able to interact. In simulations, the αE-catenin E277-R451 salt bridge is predicted

to rupture quickly under external force ([16](#), [25](#)). Unfortunately, we lack a structure of the αT-catenin M-region to determine if a similar network regulates domain organization. However, our data demonstrate that such interbundle interactions within the αT-catenin M-region are insufficient for autoinhibition.

The N-terminus is required for αT-catenin M-region autoinhibition

The αT-catenin head fragment (N1-M3) showed weak, micromolar binding to vinculin, indicating that the N-terminus regulates M-region autoinhibition. The entire N-terminus (N1-N2) is required for autoinhibition because deleting N1 restored strong vinculin binding. Notably, replacing the N-terminus with another well-structured protein moiety, the titin I27 repeats, reduced vinculin binding and caused the binding reaction to switch from exothermic to endothermic, suggesting the M1 was stabilized. This observation explains the force-dependent vinculin binding to the αT-catenin M-region observed in recent biophysical experiments ([47](#)). The ability of the titin I27 repeats to partially restore autoinhibition also suggests that steric, nonspecific interactions rather than specific interdomain associations (*e.g.*, salt bridges) between the αT-catenin N-terminus and M-region promote M1 folding and M-region autoinhibition. Interestingly, the first 56 residues of αE-catenin contribute to the inhibition of vinculin binding in addition to the M3 domain ([23](#)).

αT-catenin recruits vinculin

Expression of EGFP–αT-catenin was sufficient to restore cell–cell contacts and recruit vinculin in α-catenin-deficient R2/7 cells. Vinculin binding to αT-catenin requires actin binding by the latter and is tension dependent, similar to αE-catenin. This is consistent with the vinculin-binding site in the αT-catenin M1 domain being occluded in the absence of force. Notably, deletion of M3 in αT-catenin did not relieve autoinhibition, offering additional evidence that the intramolecular interactions required for autoinhibition in αT-catenin differ from αE-catenin.

Vinculin is recruited to αE-catenin to bolster the AJ connection to actin under mechanical load ([24](#), [33](#), [34](#), [56](#)). Neither the physiological context nor the functional role of vinculin recruitment to αT-catenin have been established *in vivo*. Loss of αE-catenin from the mouse heart disrupts AJ formation and causes a marked decrease in vinculin expression and recruitment, despite the presence of αT-catenin, resulting in cardiomyopathy ([51](#)). The inability of αT-catenin to compensate for αE-catenin in the heart underscores how the two α-catenins, despite sharing core properties, are likely regulated by distinct mechanisms and play unique roles in junction organization and signaling.

Together, our data support a model in which the αT-catenin N-terminus functions to regulate M-region stability and autoinhibition. Our *in situ* data indicate that force is required to reveal the vinculin-binding site. We speculate that it may do so by separating the M-region from the N-terminus to remove

steric hindrance rather than breaking a network of internal M-region salt bridges. This could provide cadherin–β-catenin–αT-catenin complexes in cardiomyocytes with distinct mechanical properties, allowing ligand binding and allosteric signaling over a unique force scale relative to αE-catenin-containing complexes. Although we have focused on vinculin binding to M1, intrinsic differences in αT-catenin M region organization could also affect other M1 as well as M2 and M3 ligand interactions, possibly independent of force. Intramolecular and allosteric interactions are emerging as an important factor in the regulation of α-catenin conformation and molecular complex formation at the AJ. Further work is needed to define how molecular differences between the α-catenin protein family regulate mechanical adhesion and signaling.

Experimental procedures

Plasmids

Full-length *Mus musculus* β-catenin, αT-catenin, and αE-catenin as well as αT-catenin head region (aa 1–659) in pGEX-TEV were described previously ([9](#), [12](#), [38](#)). The vinculin D1 construct (aa 1–259) in pGEX-TEV was described ([23](#)). *M. musculus* αT-catenin N1-N2 (aa 1–259), N1-M3 (aa 1–659), M1-M3 (aa 260–626), N2-M3 (aa 147–626), and αE-catenin M1-M3 (aa 273–651) and M1-M2 (aa 273–510) were cloned into pGEX-TEV. The construct encoding αT-catenin M1-M3 flanked by I27 handles in pET151/D-TOPO was kindly provided to us by Jie Yan ([47](#)).

For mammalian cell expression, full-length *M. musculus* αE-catenin and αT-catenin in pEGFP-C1 were described previously ([9](#), [38](#)). *M. musculus* αE-catenin fragments aa 1 to 670 and aa 1 to 510 and αT-catenin fragments aa 1 to 659 and aa 1 to 502 were cloned into pEGFP-C1.

Recombinant protein expression and purification

GST-tagged and His-tagged fusion proteins were expressed in BL21-Gold *E. coli* cells and purified as described ([38](#), [57](#)). GST-tagged proteins were bound to glutathione-agarose–conjugated beads, whereas His-tagged proteins were bound to Ni-NTA beads. Bound beads were then equilibrated in cleavage buffer (20-mM Tris, pH 8.0, 150-mM NaCl, 2-mM EDTA, 10% glycerol, and 1-mM DTT or BME) and incubated with tobacco etch virus protease overnight at 4 °C to cleave proteins from the respective tag. Proteins were then purified by Mono Q or Mono S ion-exchange chromatography at 4 °C, followed by S200 gel-filtration chromatography at 4 °C. Purified proteins were eluted in 20-mM Tris, pH 8.0, 150-mM NaCl, 10% glycerol, and 1-mM DTT, concentrated to working concentrations using a Millipore column concentrator and flash-frozen in liquid nitrogen.

Limited proteolysis and Edman degradation sequencing

Proteins were diluted to 12 μM in 20-mM Tris, pH 8.0, 150-mM NaCl, and 1-mM DTT and incubated at room temperature (RT) in 0.05 mg/ml sequencing grade trypsin (Roche Applied Science). Digestions were stopped with 2X Laemmli

sample buffer and placed on ice until analysis. Samples were boiled and run by SDS-PAGE and then stained with 0.1% Coomassie Brilliant Blue R-250, 40% ethanol, and 10% acetic acid. Gels were scanned on a LI-COR scanner. For N-terminal sequencing, digested peptides were blotted onto polyvinylidene difluoride membrane, stained (0.1% Coomassie Brilliant Blue R-250, 40% methanol, and 1% acetic acid), destained, and dried. Individual bands were excised from the membrane and sequenced by Edman degradation (Iowa State University Protein Facility).

Crosslinking experiments

αT-catenin protein fragments were incubated with or without 1-mM BS3 (Thermo Scientific) in 20-mM Hepes, pH 7.4, 150-mM NaCl, and 1-mM DTT for 30 min at 4 °C or 37 °C, separated by SDS-PAGE, stained with the Coomassie dye, and imaged on a LI-COR scanner.

ITC titration calorimetry

Proteins used for ITC were purified as described except the S200 buffer was replaced with the ITC buffer (20-mM Hepes, pH 8.0, 150-mM NaCl, 1-mM TCEP). An identical buffer was used to purify both cell and titrant samples to ensure buffer match. Only fresh, unfrozen proteins were used for ITC. Measurements were performed on a Malvern MicroCal PEAQ-ITC or MicroCal VP-ITC calorimeter (Malvern Panalytical). For experiments on the MicroCal PEAQ-ITC, titration occurred by an initial 0.5-μl injection followed by 18×2-μl injections of 110- to 150-μM β-catenin, 103- to 158-μM β-catenin–Ncad$_{cyto}$ complex, or 396- to 600-μM vinculin aa 1 to 259 (D1) into the cell containing 9- to 55-μM of αT-catenin or αE-catenin. For experiments on the MicroCal VP-ITC, the ligand was added with an initial 2-μl injection followed by 32×9-μl injections. The concentration of αT-catenin head or αT-catenin head–β-catenin complex in the cell varied between 22 and 56 μM. Vinculin D1 concentrations in the syringe varied between 240 and 546 μM. All calorimetry experiments were performed at 25 °C. All data analyses were performed using Malvern MicroCal ITC analysis software. For baseline correction, a mean baseline value, calculated by averaging the data points at saturation, was subtracted from each data point.

Cell culture

R2/7 carcinoma cells were cultured in Dulbecco's modified Eagle's medium (4.5 g/l glucose), 10% fetal bovine serum, 1-mM sodium pyruvate, and penicillin/streptomycin. Lipofectamine 2000 was used for all transient transfections.

Western blot

R2/7 cells were lysed 48 to 72 h after transfection in RIPA buffer (10-mM Tris, pH 7.5, 5-mM EDTA, 0.1% Triton-X 100, 0.1% SDS, 0.1% deoxycholate, 150-mM NaCl) plus protease inhibitors (Millipore). The lysate protein concentration was measured by bicinchoninic acid protein assay, and 15 μg of each sample was separated by SDS-PAGE and transferred onto a polyvinylidene difluoride membrane (Bio-Rad). The membrane was blocked in TBST (Tris-buffered saline, 0.1% TWEEN 20) + 5% BSA (bovine serum albumin) for 1 h at RT, washed in TBST, and incubated with anti-GFP (1:1000, Invitrogen A11122) and anti-GAPDH (1:500, Millipore MAB374) antibodies for 1 h at RT. The membrane was washed twice in TBST and then incubated with anti-rabbit IRDye 680 and anti-mouse IRDye 800 for 1 h at RT, washed twice with TBST, and washed once with PBS. Membranes were scanned on a Bio-Rad ChemiDoc MP imaging system.

Immunostaining and confocal microscopy

Cells were fixed in 4% paraformaldehyde in PHEM buffer (60-mM Pipes, pH 7.0, 25-mM Hepes, pH 7.0, 10-mM EGTA, pH 8.0, 2-mM MgCl, and 0.12 M sucrose), washed with PBS, permeabilized with 0.2% Triton X-100 in PBS for 2 min, and then blocked for 1 h at RT in PBS +10% BSA. Samples were washed three times in PBS, incubated with the primary antibody in PBS +1% BSA for 1 h at RT, washed three times in PBS, incubated with the secondary antibody in PBS +1% BSA for 1 h at RT, washed three times in PBS, and mounted on the ProLong Diamond mounting medium. Cells were imaged on a Nikon Eclipse Ti inverted microscope outfitted with a Prairie swept-field confocal scanner, Agilent monolithic laser launch, and Andor iXon3 camera using NIS-Elements imaging software.

Image analysis

To quantify vinculin recruitment to EGFP-tagged αE-catenin and αT-catenin, a maximum projection was created from four planes of the z-stack (600-nm total distance) where cell–cell contacts were best in focus. IsoJ Dark thresholding was used to create a mask of the GFP channel to define the region of analysis in ImageJ. Vinculin signal intensity was then measured within the masked region. Next, three random intensity measurements of vinculin staining were taken in the cell cytoplasm and these values averaged. Finally, the vinculin intensity within the mask was divided by the cytoplasmic signal to normalize between samples and calculate the contact/cytoplasmic ratio. Colocalization data were plotted with Prism software (GraphPad). A one-way ANOVA with Tukey's comparisons was performed to determine significance; $p < 0.05$.

To examine the relationship between EGPF–αE-catenin or EGFP–αT-catenin levels and vinculin recruitment, the vinculin contact/cytoplasmic ratio was plotted against the average GFP intensity of each fusion construct within the masked cell contact region (described above). Linear regression analysis was performed to calculate the slope, 95% confidence intervals, R^2 value, and p value using Prism software (GraphPad).

Data availability

All data are contained within the article.

Abbreviations—The abbreviations used are: αE, epithelial; αN, neuronal; αT, testes; ABD, F-actin binding domain; AJ, adherens junction; BS3, bis(sulfosuccinimidyl)suberate; BSA, bovine serum albumin; EGFP, enhanced green fluorescent protein; ICD, intercalated disc; ITC, isothermal titration calorimetry; M, middle; Ncad$_{cyto}$, N-cadherin tail; TBST, Tris-buffered saline, 0.1% TWEEN 20.

References

1. Ratheesh, A., and Yap, A. S. (2012) A bigger picture: Classical cadherins and the dynamic actin cytoskeleton. *Nat. Rev. Mol. Cell Biol.* **13**, 673–679
2. Rubsam, M., Broussard, J. A., Wickstrom, S. A., Nekrasova, O., Green, K. J., and Niessen, C. M. (2018) Adherens junctions and desmosomes coordinate mechanics and signaling to orchestrate tissue morphogenesis and function: An evolutionary perspective. *Cold Spring Harb. Perspect. Biol.* **10**, a029207
3. Mege, R. M., and Ishiyama, N. (2017) Integration of cadherin adhesion and cytoskeleton at adherens junctions. *Cold Spring Harb. Perspect. Biol.* **9**, a028738
4. Priest, A. V., Shafraz, O., and Sivasankar, S. (2017) Biophysical basis of cadherin mediated cell-cell adhesion. *Exp. Cell Res.* **358**, 10–13
5. Shapiro, L., and Weis, W. I. (2009) Structure and biochemistry of cadherins and catenins. *Cold Spring Harb. Perspect. Biol.* **1**, a003053
6. Meng, W. X., and Takeichi, M. (2009) Adherens junction: Molecular architecture and regulation. *Cold Spring Harb. Perspect. Biol.* **1**, a002899
7. Maiden, S. L., and Hardin, J. (2011) The secret life of alpha-catenin: Moonlighting in morphogenesis. *J. Cell Biol.* **195**, 543–552
8. Rimm, D. L., Koslov, E. R., Kebriaei, P., Cianci, C. D., and Morrow, J. S. (1995) Alpha 1(E)-catenin is an actin-binding and -bundling protein mediating the attachment of F-actin to the membrane adhesion complex. *Proc. Natl. Acad. Sci. U. S. A.* **92**, 8813–8817
9. Yamada, S., Pokutta, S., Drees, F., Weis, W. I., and Nelson, W. J. (2005) Deconstructing the cadherin-catenin-actin complex. *Cell* **123**, 889–901
10. Drees, F., Pokutta, S., Yamada, S., Nelson, W. J., and Weis, W. I. (2005) Alpha-catenin is a molecular switch that binds E-cadherin-beta-catenin and regulates actin-filament assembly. *Cell* **123**, 903–915
11. Buckley, C. D., Tan, J., Anderson, K. L., Hanein, D., Volkmann, N., Weis, W. I., Nelson, W. J., and Dunn, A. R. (2014) Cell adhesion. The minimal cadherin-catenin complex binds to actin filaments under force. *Science* **346**, 1254211
12. Pokutta, S., Choi, H. J., Ahlsen, G., Hansen, S. D., and Weis, W. I. (2014) Structural and thermodynamic characterization of cadherin.beta-catenin. alpha-catenin complex formation. *J. Biol. Chem.* **289**, 13589–13601
13. Ishiyama, N., Sarpal, R., Wood, M. N., Barrick, S. K., Nishikawa, T., Hayashi, H., Kobb, A. B., Flozak, A. S., Yemelyanov, A., Fernandez-Gonzalez, R., Yonemura, S., Leckband, D. E., Gottardi, C. J., Tepass, U., and Ikura, M. (2018) Force-dependent allostery of the alpha-catenin actin-binding domain controls adherens junction dynamics and functions. *Nat. Commun.* **9**, 5121
14. Ishiyama, N., Tanaka, N., Abe, K., Yang, Y. J., Abbas, Y. M., Umitsu, M., Nagar, B., Bueler, S. A., Rubinstein, J. L., Takeichi, M., and Ikura, M. (2013) An autoinhibited structure of alpha-catenin and its implications for vinculin recruitment to adherens junctions. *J. Biol. Chem.* **288**, 15913–15925
15. Rangarajan, E. S., and Izard, T. (2013) Dimer asymmetry defines alpha-catenin interactions. *Nat. Struct. Mol. Biol.* **20**, 188–193
16. Terekhova, K., Pokutta, S., Kee, Y. S., Li, J., Tajkhorshid, E., Fuller, G., Dunn, A. R., and Weis, W. I. (2019) Binding partner- and force-promoted changes in alphaE-catenin conformation probed by native cysteine labeling. *Sci. Rep.* **9**, 15375
17. Nieset, J. E., Redfield, A. R., Jin, F., Knudsen, K. A., Johnson, K. R., and Wheelock, M. J. (1997) Characterization of the interactions of alpha-catenin with alpha-actinin and beta-catenin/plakoglobin. *J. Cell Sci.* **110**(Pt 8), 1013–1022
18. Koslov, E. R., Maupin, P., Pradhan, D., Morrow, J. S., and Rimm, D. L. (1997) Alpha-catenin can form asymmetric homodimeric complexes and/or heterodimeric complexes with beta-catenin. *J. Biol. Chem.* **272**, 27301–27306
19. Pokutta, S., and Weis, W. I. (2000) Structure of the dimerization and beta-catenin-binding region of alpha-catenin. *Mol. Cell* **5**, 533–543
20. Imamura, Y., Itoh, M., Maeno, Y., Tsukita, S., and Nagafuchi, A. (1999) Functional domains of alpha-catenin required for the strong state of cadherin-based cell adhesion. *J. Cell Biol.* **144**, 1311–1322
21. Pokutta, S., Drees, F., Takai, Y., Nelson, W. J., and Weis, W. I. (2002) Biochemical and structural definition of the l-afadin- and actin-binding sites of alpha-catenin. *J. Biol. Chem.* **277**, 18868–18874
22. Yang, J., Dokurno, P., Tonks, N. K., and Barford, D. (2001) Crystal structure of the M-fragment of alpha-catenin: Implications for modulation of cell adhesion. *EMBO J.* **20**, 3645–3656
23. Choi, H. J., Pokutta, S., Cadwell, G. W., Bobkov, A. A., Bankston, L. A., Liddington, R. C., and Weis, W. I. (2012) AlphaE-catenin is an autoinhibited molecule that coactivates vinculin. *Proc. Natl. Acad. Sci. U. S. A.* **109**, 8576–8581
24. Yonemura, S., Wada, Y., Watanabe, T., Nagafuchi, A., and Shibata, M. (2010) Alpha-catenin as a tension transducer that induces adherens junction development. *Nat. Cell Biol.* **12**, 533–542
25. Li, J., Newhall, J., Ishiyama, N., Gottardi, C., Ikura, M., Leckband, D. E., and Tajkhorshid, E. (2015) Structural determinants of the mechanical stability of alpha-catenin. *J. Biol. Chem.* **290**, 18890–18903
26. Xu, X. P., Pokutta, S., Torres, M., Swift, M. F., Hanein, D., Volkmann, N., and Weis, W. I. (2020) Structural basis of alphaE-catenin-F-actin catch bond behavior. *Elife* **9**, e60878
27. Mei, L., Espinosa de Los Reyes, S., Reynolds, M. J., Leicher, R., Liu, S., and Alushin, G. M. (2020) Molecular mechanism for direct actin force-sensing by alpha-catenin. *Elife* **9**, e62514
28. le Duc, Q., Shi, Q., Blonk, I., Sonnenberg, A., Wang, N., Leckband, D., and de Rooij, J. (2010) Vinculin potentiates E-cadherin mechanosensing and is recruited to actin-anchored sites within adherens junctions in a myosin II-dependent manner. *J. Cell Biol.* **189**, 1107–1115
29. Yao, M., Qiu, W., Liu, R., Efremov, A. K., Cong, P., Seddiki, R., Payre, M., Lim, C. T., Ladoux, B., Mege, R. M., and Yan, J. (2014) Force-dependent conformational switch of alpha-catenin controls vinculin binding. *Nat. Commun.* **5**, 4525
30. Barrick, S., Li, J., Kong, X. Y., Ray, A., Tajkhorshid, E., and Leckband, D. (2018) Salt bridges gate alpha-catenin activation at intercellular junctions. *Mol. Biol. Cell* **29**, 111–122
31. Maki, K., Han, S. W., Hirano, Y., Yonemura, S., Hakoshima, T., and Adachi, T. (2016) Mechano-adaptive sensory mechanism of alpha-catenin under tension. *Sci. Rep.* **6**, 24878
32. Maki, K., Han, S. W., Hirano, Y., Yonemura, S., Hakoshima, T., and Adachi, T. (2018) Real-time TIRF observation of vinculin recruitment to stretched alpha-catenin by AFM. *Sci. Rep.* **8**, 1575

33. Twiss, F., Le Duc, Q., Van Der Horst, S., Tabdili, H., Van Der Krogt, G., Wang, N., Rehmann, H., Huveneers, S., Leckband, D. E., and De Rooij, J. (2012) Vinculin-dependent cadherin mechanosensing regulates efficient epithelial barrier formation. *Biol. Open* **1**, 1128–1140

34. Merkel, C. D., Li, Y., Raza, Q., Stolz, D. B., and Kwiatkowski, A. V. (2019) Vinculin anchors contractile actin to the cardiomyocyte adherens junction. *Mol. Biol. Cell* **30**, 2639–2650

35. Thomas, W. A., Boscher, C., Chu, Y. S., Cuvelier, D., Martinez-Rico, C., Seddiki, R., Heysch, J., Ladoux, B., Thiery, J. P., Mege, R. M., and Dufour, S. (2013) Alpha-catenin and vinculin cooperate to promote high E-cadherin-based adhesion strength. *J. Biol. Chem.* **288**, 4957–4969

36. Zhao, Z. M., Reynolds, A. B., and Gaucher, E. A. (2011) The evolutionary history of the catenin gene family during metazoan evolution. *BMC Evol. Biol.* **11**, 198

37. Hulpiau, P., Gul, I. S., and van Roy, F. (2013) New insights into the evolution of metazoan cadherins and catenins. *Prog. Mol. Biol. Transl.* **116**, 71–94

38. Wickline, E. D., Dale, I. W., Merkel, C. D., Heier, J. A., Stolz, D. B., and Kwiatkowski, A. V. (2016) AlphaT-catenin is a constitutive actin-binding alpha-catenin that directly couples the Cadherin.Catenin complex to actin filaments. *J. Biol. Chem.* **291**, 15687–15699

39. Janssens, B., Goossens, S., Staes, K., Gilbert, B., van Hengel, J., Colpaert, C., Bruyneel, E., Mareel, M., and van Roy, F. (2001) AlphaT-catenin: A novel tissue-specific beta-catenin-binding protein mediating strong cell-cell adhesion. *J. Cell Sci.* **114**, 3177–3188

40. Chiarella, S. E., Rabin, E. E., Ostilla, L. A., Flozak, A. S., and Gottardi, C. J. (2018) AlphaT-catenin: A developmentally dispensable, disease-linked member of the alpha-catenin family. *Tissue Barriers* **6**, e1463896

41. Goossens, S., Janssens, B., Bonne, S., De Rycke, R., Braet, F., van Hengel, J., and van Roy, F. (2007) A unique and specific interaction between alphaT-catenin and plakophilin-2 in the area composita, the mixed-type junctional structure of cardiac intercalated discs. *J. Cell Sci.* **120**, 2126–2136

42. Vite, A., and Radice, G. L. (2014) N-cadherin/catenin complex as a master regulator of intercalated disc function. *Cell Commun. Adhes.* **21**, 169–179

43. Li, J., Goossens, S., van Hengel, J., Gao, E., Cheng, L., Tyberghein, K., Shang, X., De Rycke, R., van Roy, F., and Radice, G. L. (2012) Loss of alphaT-catenin alters the hybrid adhering junctions in the heart and leads to dilated cardiomyopathy and ventricular arrhythmia following acute ischemia. *J. Cell Sci.* **125**, 1058–1067

44. van Hengel, J., Calore, M., Bauce, B., Dazzo, E., Mazzotti, E., De Bortoli, M., Lorenzon, A., Li Mura, I. E., Beffagna, G., Rigato, I., Vleeschouwers, M., Tyberghein, K., Hulpiau, P., van Hamme, E., Zaglia, T., *et al*. (2013) Mutations in the area composita protein alphaT-catenin are associated with arrhythmogenic right ventricular cardiomyopathy. *Eur. Heart J.* **34**, 201–210

45. Folmsbee, S. S., Morales-Nebreda, L., Van Hengel, J., Tyberghein, K., Van Roy, F., Budinger, G. R., Bryce, P. J., and Gottardi, C. J. (2015) The cardiac protein alphaT-catenin contributes to chemical-induced asthma. *Am. J. Physiol. Lung Cell Mol. Physiol.* **308**, L253–258

46. Folmsbee, S. S., Wilcox, D. R., Tyberghein, K., De Bleser, P., Tourtellotte, W. G., van Hengel, J., van Roy, F., and Gottardi, C. J. (2016) AlphaT-catenin in restricted brain cell types and its potential connection to autism. *J. Mol. Psychiatry* **4**, 2

47. Pang, S. M., Le, S., Kwiatkowski, A. V., and Yan, J. (2019) Mechanical stability of alphaT-catenin and its activation by force for vinculin binding. *Mol. Biol. Cell* **30**, 1930–1937

48. Kostetskii, I., Li, J., Xiong, Y., Zhou, R., Ferrari, V. A., Patel, V. V., Molkentin, J. D., and Radice, G. L. (2005) Induced deletion of the N-cadherin gene in the heart leads to dissolution of the intercalated disc structure. *Circ. Res.* **96**, 346–354

49. Watabe-Uchida, M., Uchida, N., Imamura, Y., Nagafuchi, A., Fujimoto, K., Uemura, T., Vermeulen, S., van Roy, F., Adamson, E. D., and Takeichi, M. (1998) Alpha-catenin-vinculin interaction functions to organize the apical junctional complex in epithelial cells. *J. Cell Biol.* **142**, 847–857

50. Li, Y., Merkel, C. D., Zeng, X., Heier, J. A., Cantrell, P. S., Sun, M., Stolz, D. B., Watkins, S. C., Yates, N. A., and Kwiatkowski, A. V. (2019) The N-cadherin interactome in primary cardiomyocytes as defined using quantitative proximity proteomics. *J. Cell Sci.* **132**, jcs221606

51. Sheikh, F., Chen, Y., Liang, X., Hirschy, A., Stenbit, A. E., Gu, Y., Dalton, N. D., Yajima, T., Lu, Y., Knowlton, K. U., Peterson, K. L., Perriard, J. C., and Chen, J. (2006) Alpha-E-catenin inactivation disrupts the cardiomyocyte adherens junction, resulting in cardiomyopathy and susceptibility to wall rupture. *Circulation* **114**, 1046–1055

52. Kowalczyk, A. P., and Green, K. J. (2013) Structure, function, and regulation of desmosomes. *Prog. Mol. Biol. Transl. Sci.* **116**, 95–118

53. Choi, H. J., Gross, J. C., Pokutta, S., and Weis, W. I. (2009) Interactions of plakoglobin and beta-catenin with desmosomal cadherins: Basis of selective exclusion of alpha- and beta-catenin from desmosomes. *J. Biol. Chem.* **284**, 31776–31788

54. Benjamin, J. M., Kwiatkowski, A. V., Yang, C., Korobova, F., Pokutta, S., Svitkina, T., Weis, W. I., and Nelson, W. J. (2010) AlphaE-catenin regulates actin dynamics independently of cadherin-mediated cell-cell adhesion. *J. Cell Biol.* **189**, 339–352

55. Wood, M. N., Ishiyama, N., Singaram, I., Chung, C. M., Flozak, A. S., Yemelyanov, A., Ikura, M., Cho, W., and Gottardi, C. J. (2017) Alpha-catenin homodimers are recruited to phosphoinositide-activated membranes to promote adhesion. *J. Cell Biol.* **216**, 3767–3783

56. Huveneers, S., Oldenburg, J., Spanjaard, E., van der Krogt, G., Grigoriev, I., Akhmanova, A., Rehmann, H., and de Rooij, J. (2012) Vinculin associates with endothelial VE-cadherin junctions to control force-dependent remodeling. *J. Cell Biol.* **196**, 641–652

57. Hansen, S. D., Kwiatkowski, A. V., Ouyang, C. Y., Liu, H., Pokutta, S., Watkins, S. C., Volkmann, N., Hanein, D., Weis, W. I., Mullins, R. D., and Nelson, W. J. (2013) AlphaE-catenin actin-binding domain alters actin filament conformation and regulates binding of nucleation and disassembly factors. *Mol. Biol. Cell* **24**, 3710–3720

ASBMB